Published in final edited form as:

J Phys Chem B. 2015 February 5; 119(5): 1787–1792. doi:10.1021/jp508710g.

Low-Temperature Polymorphic Phase Transition in a Crystalline Tripeptide L-Ala-L-Pro-Gly·H_2O Revealed by Adiabatic Calorimetry

Alexey V. Markin[*,†,§], **Evgeny Markhasin**[‡,§], **Semen S. Sologubov**[†], **Qing Zhe Ni**[‡], **Natalia N. Smirnova**[†], and **Robert G. Griffin**[‡]

[†]Lobachevsky State University of Nizhny Novgorod, Gagarin Pr. 23/5, Nizhny Novgorod 603950, Russia

[‡]Massachusetts Institute of Technology, 150 Albany Street, Cambridge, Massachusetts 02139, United States

Abstract

We demonstrate application of precise adiabatic vacuun calorimetry to observation of phase transition in the tripeptide L-alanyl-L-prolyl-glycine monohydrate (APG) from 6 to 320 K and report the standard thermodynamic properties of the tripeptide in the entire range. Thus, the heat capacity of APG was measured by adiabatic vacuun calorimetry in the above temperature range. The tripeptide exhibits a reversible first-order solid-to-solid phase transition characterized by strong thermal hysteresis. We report the standard thermodynamic characteristics of this transition and show that differential scanning calorimetry can reliably characterize the observed phase transition with <5 mg of the sample. Additionally, the standard entropy of formation from the elemental substances and the standard entropy of hypothetical reaction of synthesis from the amino acids at 298.15 K were calculated for the studied tripeptide.

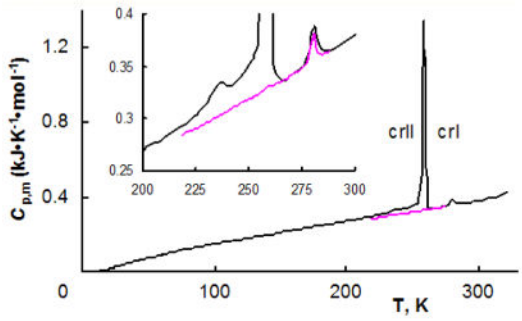

INTRODUCTION

Partial or complete structural elucidation of the atomic level structure of biological molecules, such as peptides and proteins, is essential for subsequent investigation of their function and disfunction. Structural information at the atomic level is primarily provided by

[*]**Corresponding Author** Fax: +7 831 462 31 55. markin@calorimetry-center.ru..

[§]A.V.M. and E.M. contributed equally.

The authors declare no competing financial interest

diffraction and magnetic resonance techniques. Because both techniques can benefit from low temperatures, these experiments are often performed on cryogenically cooled samples. Furthermore, certain techniques, such as dynamic nuclear polarization (DNP)[1,2] in combination with cryogenic magic-angle spinning (MAS)[3] nuclear magnetic resonance (NMR), provide valuable information, which may not be otherwise available. At the same time, it is the ambient temperature structure, which is of interest[4–7]

Calorimetric techniques, such as differential scanning calorimetry (DSC) or adiabatic calorimetry, are particularly suitable for probing temperature-dependent changes in structure, including polymorphism[8–10] and glass-like transitions.[5,11–15] If phase transformations, irreversible changes, or inadequate reproducibility cannot be detected in calorimetric experiments, the low-temperature spectroscopic data are likely to be relevant. Additionally, calorimetric information is also valuable for thermodynamic analysis of processes and thermodynamic databanks.[16]

Canonical amino acids or their common derivatives and small peptides are two classes of relatively simple molecules conventionally used for methods development aimed at biological objects. Several such model molecules have been routinely used in the Griffin Lab. Low-temperature thermodynamic properties are available for most of the canonical amino acids,[8-10,18-31] as well as a number of other biological molecules,[17] including short peptides[32–36] and even proteins.[11,15,37–40] Most of these works report relatively monotonic heat capacity dependence without well-pronounced phase transitions, and additive behavior of heat capacity in a wide range of temperatures.[34,36] The present work was motivated by a variety of spectral changes observed in variable temperature MAS NMR spectra of two model tripeptides, APG (Ni et al., in preparation) and N-formyl-L-Met-L-Leu-L-Phe (N-f-MLF–OH).41 Our previous investigation of MLF–OH that exhibits similar peculiarities in the NMR data[41] did not reveal any phase transitions.[36] Thus, the purposes of the present study included the extension of that investigation to APG using adiabatic calorimetry and DSC, detection of possible phase transitions and their thermodynamic characteristics, and obtaining the standard thermodynamic properties of the tripeptide in a wide temperature range from 6 to 320 K.

EXPERIMENTAL SECTION

Synthesis and Characterization of the Tripeptide

Tripeptide Ala-Pro-Gly (lot 0513046) was purchased from Bachem (King of Prussia, PA) and recrystallized from water. The crystal structure of the sample (space group $P2_12_12_1$, $Z = 4$[42,43] was confirmed by single-crystal X-ray diffraction (Siemens three-circle Platform diffractometer) and by powder X-ray diffraction (PANalytical X-'Pert Pro multipurpose diffractometer equipped with Oxford Cryosystems PheniX cryostat). The sample purity was >99% (TLC) and in accordance with elemental analysis for anhydrous tripeptide ($C_{10}H_{17}N_3O_4$), found/calculated (mass %): C 46.09/45.97, H 7.27/7.33, N 16.01/16.08.

Adiabatic Calorimetry

A precision adiabatic calorimeter (Block Calorimetric Thermophysical, BCT-3) was used to measure heat capacities over the temperature range from 6 to 320 K. The design and

operation of an adiabatic calorimeter are described in detail elsewhere.[44,45] A calorimetric cell is a thin-walled cylindrical vessel made from titanium with a volume of 1.5×10^{-6} m^3 and mass of 1.626 ± 0.005 g. A miniature iron–rhodium resistance thermometer (nominal resistance 100 Ω; calibrated on ITS-90 standard by the Russian Metrology Research Institute, Moscow region, Russia) was used to measure the temperature of the sample. The temperature difference between the ampule and an adiabatic shield was controlled by a four-junction copper–iron chromel thermo-couple. The sensitivity of the thermometric circuit was 1×10^{-3} K and that of the analog-to-digital converter was 0.1 μV. The accuracy of the calorimeter was verified using standard reference samples (K-2 benzoic acid and α-Al_2O_3)[46,47] prepared by the Institute of Metrology of the State Standard Committee of the Russian Federation. The deviations of our results from the recommended values of NIST[46] are within 0.02 $C_{p,m}$ between 6 and 20 K, 0.005 $C_{p,m}$ between 20 and 40 K, and 0.002 $C_{p,m}$ between 40 and 320 K. The standard uncertainty for the temperature was $u(T) = 0.01$ K, and the relative standard uncertainty for the enthalpies of transitions was $u_r(\Delta_{tr}H) = 0.002$.

Differential Scanning Calorimetry

DSC experiments were conducted on a differential scanning calorimeter DSC 204 *Fl Phoenix,* Netzsch–Gerätebau, Germany. The calorimeter was calibrated and tested against melting of *n*-heptane, mercury, tin, lead, bismuth, and zinc. The standard uncertainty for temperature was $u(T) = 0.5$ K, and the relative standard uncertainty for enthalpies of transitions was $u_r(\Delta_{tr}H) = 0.01$. The measurements were carried out in an argon atmosphere in accordance with protocols described elsewhere.[48,49]

Heat Capacity Measurements

A sample of tripeptide (0.1991 g) was placed in a calorimetric ampule, which was then filled with dry helium gas to the pressure of 4 kPa at room temperature to facilitate heat transfer. Initially, the sample was cooled to the temperature of the measurement onset (~6 K) at a rate of 0.01 K/s. Then, the sample was heated in 0.5 to 2 K increments at a rate of 0.01 K/s. The sample temperature was recorded after an equilibration period (temperature drift <0.01 $K \cdot s^{-1}$, ~10 min per experimental point).

The experimental values of $C_{p,m}$ were obtained in four series reflecting the sequence of experiments. The heat capacity of the sample was between 15 and 50% of the overall heat capacity of the calorimetric ampule with the substance within the studied temperature range.

The experimental data were smoothed using least-squares polynomial fits as follows

$$C_{p,m} = \begin{cases} \sum_{i=0}^{7} A_i \quad ln\left(\frac{T}{30}\right)^i, \\ 6 \le T \le 40 \quad \mathrm{K} \\ \sum_{i=0}^{6} B_i \quad ln\left(\frac{T}{30}\right)^i, \\ 40 \le T \le 320 \quad \mathrm{K} \end{cases}$$

where A_i and B_i are polynomial coefficients. Smoothing of the experimental values of $C_{p,m}$ was performed over the whole temperature range excluding the intervals of phase

transitions. The relative standard uncertainty of heat capacity $u_r(C_{p,m})$ is 0.006 and 0.003 in temperature ranges $6 \leq T \leq 40$ K and $40 \leq T \leq 320$ K, respectively.

The molar mass of L-Ala-L-Pro-Gly·H_2O (261.28 g·mol^{-1}) was calculated from the International Union of Pure and Applied Chemistry (IUPAC) table of atomic weights.[50]

RESULTS AND DISCUSSION

Heat Capacity and Thermodynamic Characteristics of Phase Transition

Experimental molar heat capacity $C_{p,m}$ of L-Ala-L-Pro-Gly·H_2O over the temperature range from 6 to 320 K is presented in Figure 1. There are two regions in which heat capacity changes nonmonotonically.

The strong peak in the range of 226 to 265 K is characteristic of a first-order phase transition, which is assigned to a polymorphic solid-to-solid phase transition (crII ↔ crI). The anomaly between 275 and 287 K is attributed to excitation of rotational degrees of freedom. Both of these features were well-reproducible in all experiments, and their standard thermodynamic properties obtained using adiabatic vacuum calorimetry are presented in Table 1.

The crI ↔ crI phase transition exhibits strong thermal hysteresis, and upon slow cooling (0.05 K/s) the high-temperature phase crI could be supercooled to ~210 K (pink trace in Figure 1). Further cooling of the sample was accompanied by heat liberation associated with the transformation of the metastable phase crI to the stable phase crII. This supercooling phenomenon was also clearly observed in a single-crystal X-ray diffraction study, where single-crystal disintegration occurred in the same temperature range (Figure 2). All X-ray attempts to cool a single crystal of APG eventually resulted in full disintegration of the sample, sometimes in an explosive manner, indicating significant changes in the crystal structure. The strong thermal hysteresis is, in turn, consistent with a large activation barrier separating two significantly different crystal structures. Present result can thus be contrasted with the previously studied tripeptide N-*f*-MLF–OH.[36] While both exhibit similar anomalies in the temperature-dependent MAS NMR spectra involving line doubling, calorimetric experiment established that no phase transitions occurred in the case of N-*f*-MLF–OH.

While adiabatic vacuum calorimetry is a reliable and precise method of investigation of polymorphic phase transitions in different materials, including peptides and proteins, it requires a relatively large sample size, thus limiting its application to mass limited biomolecules. DSC is less precise but can be used to study smaller samples. To test its limits, we applied DSC to characterization of the polymorphic phase transition crII ↔ crI using two small samples (10.6 and 4.7 mg) and compared the obtained thermodynamic properties with the result of adiabatic vacuum calorimetry. Figure 3 shows the DSC traces for the two studied samples, and the corresponding thermodynamic properties of the phase transition are presented in Table 2. The enthalpy of transition, transition temperature, and temperature range agree with each other for the two experiments and are within the experimental error compared with the values obtained by adiabatic vacuum calorimetry

(Table 1). Therefore, DSC should be suitable for characterization of polymorphic phase transitions in peptides and, possibly, other biomolecules using several milligrams of sample.

Low-temperature heat capacity data were also analyzed using the multifractal model[51]

$$C_\nu = 3D\,(D+1)\,kN\gamma\,(D+1)\,\zeta\,(D+1)\left(\frac{T}{\Theta_{max}}\right)^{\mathrm{D}} \quad (1)$$

where D is the fractal dimension, N is the number of atoms in a molecular unit, k is the Boltzmann constant, γ is the γ function, ξ is the Riemann ξ function, and Θ_{max} is the characteristic temperature. For a particular solid, $3D(D + 1)kN\gamma(D + 1)\zeta(D + 1) = A$ is a constant, and eq 1 can be rewritten as follows

$$ln\,(C_\nu) = A + D \quad ln\,(T) \quad (2)$$

which can be used to obtain D and Θ_{max}. Because below 50 K $C_p \approx C_\nu$, experimental data in the range $20 \le T \le 50$ K were used. We obtained $\Theta_{max} = 252.0$ K (relative standard uncertainty $u_r(\Theta_{max}) = 0.007$) and $D = 2$, which according to the fractal model[51] corresponds to a layered structure.

Standard Thermodynamic Functions

The Debye theory[52] was used to fit the experimental data in the range $6 \le T \le 12$ K and extrapolate it to 0 K

$$C_{p,\mathrm{m}} = nD\left(\frac{\Theta_{\mathrm{D}}}{T}\right) \quad (3)$$

where D is the Debye function and n and Θ_{D} are fitting parameters. Using this equation, we obtained $n = 6$, $\Theta_{\mathrm{D}} = 130.5$ K, and the relative standard uncertainty of the fit $u_r(C_{p,\mathrm{m}}) = 0.013$ for $6 \le T \le 12$ K. In subsequent calculations, we assumed that the relative standard uncertainty of the extrapolated $C_{p,\mathrm{m}}$ to $T = 0$ K was the same.

$H(T) - H(0)$ and $S(T)$ were calculated by numerical integration of $C_{p,\mathrm{m}}$ with respect to T and ln T, respectively, and Gibbs energy was calculated from enthalpy and entropy following published procedures.[53] The residual entropy of L-Ala-L-Pro-Gly·H_2O was assumed to be zero (Table 3). The standard entropies of the tripeptide and elemental substances, including carbon,[54] hydrogen,[55] nitrogen,[54] and oxygen,[55] yielded the standard entropy of formation

$$10\mathrm{C}\,(gr) + 19/2\mathrm{H_2}\,(\mathrm{g}) + 3/2\mathrm{N_2}\,(\mathrm{g}) + 5/2\mathrm{O_2}\,(\mathrm{g}) \rightarrow \mathrm{C_{10}H_{19}N_3O_5}\,(cr)$$

$$\Delta_f S\,(298.15\mathrm{K}, \quad \mathrm{L} - Ala - \mathrm{L} - Pro - Gly \cdot \mathrm{H_2O}, \quad cr) = -1705 \pm 17 \quad \mathrm{J{\cdot}K^{-1}{\cdot}}mol^{-1}$$

where cr, gr, and g are crystal, graphite, and gas, respectively. The standard entropies of amino acids, including alanine,[31] proline,[28] and glycine,[27] also yielded the standard entropy of synthesis of the tripeptide from individual amino acids

$$\mathrm{L}-Ala\,(cr)+\mathrm{L}-Pro\,(cr)+Gly\,(cr)\leftrightarrow\quad \mathrm{L}-Ala-\mathrm{L}-Pro-Gly\cdot\mathrm{H_2O}\,(cr)+\mathrm{H_2O}\,(1)$$

$$\Delta_{\mathrm{r}}S\,(298.15\quad \mathrm{K})=77.96\pm 0.78\quad \mathrm{J}\cdot\mathrm{K}^{-1}\cdot mol^{-1}$$

The formation of a complex molecule (tripeptide) from several simpler molecules (amino acids) usually results in reduction of entropy. The positive change of entropy in this process indicates that the formation of another small molecule (water) in the liquid state outweighs the loss of entropy due to formation of a larger molecule. The overall magnitude of entropy change is relatively small and the Gibbs energy of the reaction is likely to be dominated by the enthalpy contribution.

CONCLUSIONS

Adiabatic vacuum calorimetry revealed a well-defined first-order polymorphic phase transition in a crystalline tripeptide L-Ala-L-Pro-Gly·H_2O. This transition exhibits a strong thermal hysteresis, and the high-temperature phase can be readily supercooled by ~50 K. The supercooling phenomenon was also observed in single-crystal X-ray experiments. Because of the polymorphic transition in this situation, structural information obtained at cryogenic temperatures is likely to be irrelevant to the room temperature structure.

In DSC experiments, the same transition was accurately reproduced with <5 mg of sample. The standard thermodynamic characteristics of the phase transition were independently determined by both adiabatic calorimetry and DSC, and the obtained values were within the experimental error. Thus, it should be possible to apply DSC to the investigation of small biological samples, although additional verification on other model systems is desirable.

Heat capacity of the peptide was measured over the range from 6 to 320 K by precise adiabatic vacuum calorimetry. Standard thermodynamic functions of the tripeptide were calculated over the range from 0 to 320 K. The standard entropies of formation of the tripeptide from elemental substances and individual amino acids have also been reported.

The low-temperature ($T \leq 50$ K) heat capacity was analyzed using Debye's theory of heat capacity and its multifractal model, and a layered structure topology was established for the studied tripeptide.

The next stage should involve application of calorimetry to other objects, such as model amyloidogenic peptides.

ACKNOWLEDGMENTS

We thank Dr. Peter Müller and X-ray Diffraction Facility, Department of Chemistry, MIT for collecting single crystal X-ray data.

Funding

This research was supported by the National Institute of Biomedical Imaging and Bioengineering of the National Institutes of Health through grants EB-003151, EB-001960, and EB-002026; the Ministry of Education and Science of the Russian Federation (contract no. 4.1275.2014/K). The content is solely the responsibility of the authors and does not necessarily represent the official views of the National Institutes of Health.

REFERENCES

(1). Barnes AB, De Paepe G, van der Wel PCA, Hu KN, Joo CG, Bajaj VS, Mak-Jurkauskas ML, Sirigiri JR, Henfeld J, Temkin RJ, et al. High-Field Dynamic Nuclear Polarization for Solid and Solution Biological Nmr. AppL Magn. Re.son. 2008; 34:237–263.

(2). Ni QZ, Daviso E, Can TV, Markhasin E, Jawla SK, Swager TM, Temkin RJ, Henfeld J, Griffin RG. High Frequency Dynamic Nuclear Polarization. Acc. Chem. Res. 2013; 46:1933–1941. [PubMed: 23597038]

(3). Debelouchina GT, Bayro MJ, van der Wei PCA, Caporini MA, Barnes AB, Rosay M, Maas WE, Griffin RG. Dynamic Nuclear Polarization-Enhanced Solid-State NMR Spectros-copy of GNNQQNY Nanocrystals and Amyloid Fibrils. Phys. Chem. Chem. Phys. 2010; 12:5911–5919. [PubMed: 20454733]

(4). Barnes AB, Corzilius B, Mak-Jurkauskas ML, Andreas LB, Bajaj VS, Matsuki Y, Belenky ML, Lugtenburg J, Sirigiri JR, Temkin RJ, et al. Resolution and Polarization Distribution in Cryogenic DNP/MAS Experiments. Phys. Chem. Chem. Phys. 2010; 12:5861–5867. [PubMed: 20454732]

(5). Jansson H, Bergman R, Swenson J. Role of Solvent for the Dynamics and the Glass Transition of Proteins. J. Phys. Chem. B. 2011; 115:4099–4109. [PubMed: 21425816]

(6). Ngai KL, Capaccioli S, Shinyashiki N. The Protein “Glass” Transition and the Role of the Solvent. J. Phys. Chem. B. 2008; 112:3826–3832. [PubMed: 18318525]

(7). Ringe D, Petsko GA. The “Glass Transition” In Protein Dynamics: What It Is, Why It Occurs, and How to Exploit It. Biophys. Chem. 2003; 105:667–680. [PubMed: 14499926]

(8). Minkov VS, Tumanov NA, Kolesov BA, Boldyreva EV, Bizyaev SN. Phase Transitions in the Crystals of L- and Dl-Cysteine on Cooling: The Role of the Hydrogen-Bond Distortions and the Side-Chain Motions. 2. Dl-Cysteine. J. Phys. Chem. B. 2009; 113:5262–5272. [PubMed: 19301837]

(9). Paukov IE, Kovalevskaya YA, Boldyreva EV. Low-Temperature Thermodynamic Properties of L-Cysteine. J. Therm. AnaL Calorim. 2008; 93:423–428.

(10). Paukov LE, Kovalevskaya YA, Drebushchak VA, Drebushchak TN, Boldyreva EV. An Extended Phase Transition in Crystalline L-Cysteine near 70 K. J. Phys. Chem B. 2007; 111:9186–9188. [PubMed: 17630793]

(11). Bellavia G, Cordone L, Cupane A. Calorimetric Study of Myoglobin Embedded in Trehalose-Water Matrixes. J. Therm. AnaL Calorim. 2009; 95:699–702.

(12). Doster W. The Protein-Solvent Glass Transition. Biochim. Biophys. Acta, Proteins Proteomics. 2010; 1804:3–14.

(13). Grunina NA, Belopolskaya TV, Tsereteli GI. The Glass Transition Process in Humid Biopolymers. DSC Study. J. Phys.: Conf. Ser. 2006; 40:105–110.

(14). Khodadadi S, Malkovskiy A, Kisliuk A, Sokolov AP. A Broad Glass Transition in Hydrated Proteins. Biochim. Biophys. Acta, Proteins Proteomics. 2010; 1804:15–19.

(15). Sartor G, Johari GP. Calorimetric Studies of the Kinetic Unfreezing of Molecular Motions in Hydrated Lysozyme, Hemoglo-bin, and Myoglobin. Biophys. J. 1994; 66:249–258. [PubMed: 8130342]

(16). Kutyin AM, Markhasin EM, Karyakin NV. Processing and Approximation of Calorimetric Data by the Generalized Debye Functions. Russ. J. Phys. Chem. 2004; 78:571–573.

(17). Mrevlishvili GM. Low-Temperature Calorimetry of Biological Macromolecules. Phys.-Usp. 1979; 22:433–455.

(18). Kolesov BA, Minkov VS, Boldyreva EV, Drebushchak TN. Phase Transitions in the Crystals of L- and Dl-Cysteine on Cooling: Intermolecular Hydrogen Bonds Distortions and the Side-Chain

Motions of Thiol-Groups. 1. L-Cysteine. J. Phys. Chem. B. 2008; 112:12827–12839. [PubMed: 18793012]

(19). Paukov I, Kovalevskaya Y, Boldyreva E. Low-Temperature Heat Capacity of L- and Dl Phenylglycines. J. Therm. AnaL Calorim. 2010:1–6.

(20). Paukov I, Kovalevskaya Y, Boldyreva E. Low-Temperature Thermodynamic Properties of Dl-Cysteine. J. Therm. Anal. Calorim. 2010; 100:295–301.

(21). Drebushchak V, Kovalevskaya Y, Paukov I, Boldyreva E. Low-Temperature Heat Capacity of a and γ Polymorphs of Glycine. J. Therm. Anal. Calorim. 2003; 74:109–120.

(22). Drebushchak VA, Boldyreva EV, Kovalevskaya YA, Paukov IE, Drebushchak TN. Low-Temperature Heat Capacity of β-Glycine and a Phase Transition at 252 K. J. Therm. Anal. Calorim. 2005; 79:65–70.

(23). Drebushchak VA, Kovalevskaya YA, Paukov IE, Boldyreva EV. Heat Capacity of D- and Dl-Serine in a Temperature Range of 5.5 to 300 K. J. Therm. Anal. Calorim. 2007; 89:649–654.

(24). Boldyreva EV, Chesalov YA, Drebushchak TN, Kolesnik EN, Kovalevskaya YA, Paukov IE, Drebushchak VA, Kolesov BA. Phase Transition at 204-250 K in the Crystals of β-Alanine: Kinetically Irreproduceable, or an Artefact? Phase Transitions. 2009; 82:497–506.

(25). Cole AG, Hutchens JO, Stout JW. Heat Capacities from 11 to 305 K and Entropies of L-Arginine-Hcl, L-Histidine-Hcl, and L-Lysine Hcl. J. Phys. Chem. 1963; 67:2245–2247.

(26). Hutchens JO, Cole AG, Stout JW. Heat Capacities from 11 to 305 K, Entropies, and Free Energies of Formation of L-Valine, L-Isoleucine, and L-Leucine. J. Phys. Chem. 1963; 67:1128–1130.

(27). Hutchens JO, Cole AG, Stout JW. Heat Capacities from 11 to 305 K and Entropies of L-Alanine and Glycine. J. Am. Chem. Soc. 1960; 82:4813–4815.

(28). Cole AG, Hutchens JO, Stout JW. Heat Capacities from 11 to 305 K and Entropies of L-Phenylalanine, L-Proline, L-Tryptophan, and L-Tyrosine. Some Free Energies of Formation. J. Phys. Chem. 1963; 67:1852–1855.

(29). Hutchens JO, Cole AG, Robie RA, Stout JW. Heat Capacities from 11 to 305 K, Entropies and Free Energies of Formation of L-Asparagine Monohydrate, L-Aspartic Acid, L-Glutamiic Acid, and L-Glutamine. J. BioL Chem. 1963; 238:2407–2412. [PubMed: 13955915]

(30). Hutchens JO, Cole AG, Stout JW. Heat Capacities and Entropies of L-Cystine and L-Methionine. J. BioL Chem. 1964; 239:S91–S9S.

(31). Daurel M, Delhaes P, Dupart E. Variations Thermiques, Entre 1 Et 300 K, De La Chaleur Specifique De La L-Alanine, Tri(L-Alanine), Et De La Poly(L-Alanine) Sous Formes Alpha Et Beta. Biopolymers. 1975; 14:801–823. [PubMed: 1156638]

(32). Pometun MS, Gundusharma UM, Richardson JF, Wittebort RJ. Solid State NMR and Calorimetry of Structural Waters in Helical Peptides. J. Am. Chem. Soc. 2002; 124:2345–2351. [PubMed: 11878990]

(33). Drebushchak VA, Kovalevskaya YA, Paukov IE, Boldyreva EV. Heat Capacity of α-Glycylglycine in a Temperature Range of 6 to 440 K. Comparison with Glycines. J. Therm. Anal. Calorim. 2006; 85:485–490.

(34). Drebushchak V, Kovalevskaya Y, Paukov I, Boldyreva E. Low-Temperature Heat Capacity of Diglycylglycine. J. Therm. Anal. Calorim. 2008; 93:86S–869.

(35). Hutchens JO, Cole AG, Stout JW. Heat Capacities from 11 to 305 K, Entropies, and Free Energy of Formation of Glycylglycine. J. BioL Chem. 1969; 244:33–35. [PubMed: 5773287]

(36). Markin AV, Markhasin E, Sologubov SS, Smirnova NN, Griffin RG. Standard Thermodynamic Functions of Tripeptides N-Formyl-L-Methionyl-L-Leucyl-L-Phenylalaninol and N-Formyl-L-Me thionyl-L-Leucyl-L-Phenylalanine Methyl Ester. J. Chem. Eng. Data. 2014; 59:1240–1246. [PubMed: 24803685]

(37). Hutchens JO, Cole AG, Stout JW. Heat Capacities from 11 to 305 K, and Entropies of Hydrated and Anhydrous Bovine Zinc Insulin and Bovine Chymotrypsinogen A. Entropy Change for Formation of Peptide Bonds. J. Biol Chem. 1969; 244:26–32.

(38). Bellavia G, Giuffrida S, Cottone G, Cupane A, Cordone L. Protein Thermal Denaturation and Matrix Glass Transition in Different Protein-Trehalose-Water Systems. J. Phys. Chem. B. 2011; 115:6340–6346. [PubMed: 21488647]

(39). Bellavia G, Cottone G, Giuffrida S, Cupane A, Cordone L. Thermal Denaturation of Myoglobin in Water-Disaccharide Matrixes: Relation with the Glass Transition of the System. J. Phys. Chem. B. 2009; 113:11543–11549. [PubMed: 19719261]

(40). Kawai K, Suzuki T, Oguni M. Low-Temperature Glass Transitions of Quenched and Annealed Bovine Serum Albumin Aqueous Solutions. Biophys. J. 2006; 90:3732–3738. [PubMed: 16500968]

(41). Bajaj VS, van der Wel PCA, Griffin RG. Observation of a Low-Temperature, Dynamically Driven Structural Transition in a Polypeptide by Solid-State NMR Spectroscopy. J. Am. Chem. Soc. 2009; 131:118–128. [PubMed: 19067520]

(42). Barnes AB, Andreas LB, Huber M, Ramachandran R, van der Wei PCA, Veshtort M, Griffin RG, Mehta MA. High-Resolution Solid-State NMR Structure of Alanyl-Prolyl-Glycine. J. Magn. Re.son. 2009; 200:95–100.

(43). Wu S, Declercq JP, Tinant B, Van Meerssche M. Crystal Structure and Conformation of Short Linear Peptides. Part VI. L-Alanyl L-Prolyl-Glycine Monohydrate. Bull. Soc. Chim. Belg. 1987; 96:515–520.

(44). Varushchenko RM, Druzhinina AI, Sorkin EL. Low-Temperature Heat Capacity of 1-Bromoperfluorooctane. J. Chem. Thermodyn. 1997; 29:623–637.

(45). Malyshev VM, Mil'ner GA, Sorokin EL, Shibakin VF. Automatic Low-Temperature Calorimeter. Instrum. Exp. Technol. 1985:195–197.

(46). Archer DG. Thermodynamic Properties of Synthetic Sapphire (α-Al_2O_3), Standard Reference Material 720 and the Effect of Temperature-Scale Differences on Thermodynamic Properties. J. Phys. Chem. Ref. Data. 1993; 22:1441–1453.

(47). Della Gatta G, Richardson MJ, Sarge SM, Stolen S. Standards, Calibration, and Guidelines in Microcalorimetry. Part 2. Calibration Standards for Differential Scanning Calorimetry. Pure Appl. Chem. 2006; 78:1455–1476.

(48). Drebushchak VA. Calibration Coefficient of a Heat-Flow DSC. Part II. Optimal Calibration Procedure. J. Therm. Anal. Calorim. 2005; 79:213–218.

(49). Höhne, G.; Hemminger, W.; Flammersheim, H-J. Differential Scanning Calorimetry. 2nd. Springer; New York: 2003.

(50). Coplen TB. Atomic Weights of the Elements 1999. Pure Appl. Chem. 2001; 73:667–683.

(51). Lazarev VB, Izotov AD, Gavrichev KS, Shebershneva OV. Fractal Model of Heat Capacity for Substances with Diamond-Like Structures. Thermochim. Acta. 1995; 269/270:109–116.

(52). Rabinovich, IB.; Nistratov, VP.; Telnoy, VI.; Sheiman, MS. Thermochemical and Thermodynamic Properties of Organometallic Compounds. Begell House; New York: 1999.

(53). McCullough, JP.; Scott, DW. Calorimetry of Non-Reacting Systems. Butterworth; London: 1968.

(54). Chase MWJ. Nist-Janaf Thermochemical Tables. J. Phys. Chem. Ref. Data. 1998; 9:1–1951.

(55). Cox, JD.; Wagman, DD.; Medvedev, VA. Codata Key Values for Thermodynamics. Hemisphere; New York: 1989.

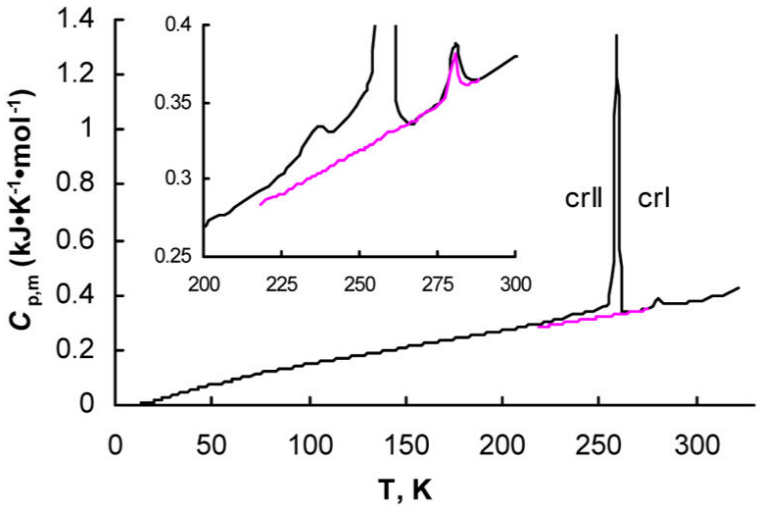

Figure 1.

Temperature dependence of the molar heat capacity $C_{p,m}$ of L-Ala-L-Pro-Gly·H_2O. Pink line corresponds to a metastable state.

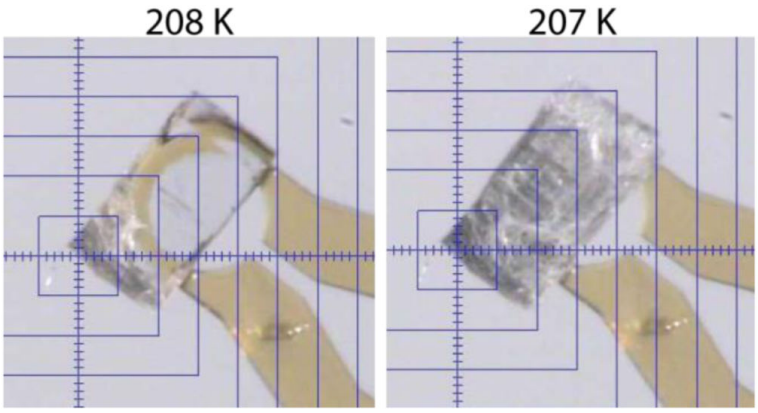

Figure 2.
Photographs showing a supercooled single crystal of APG fracturing due to a polymorphic phase transition.

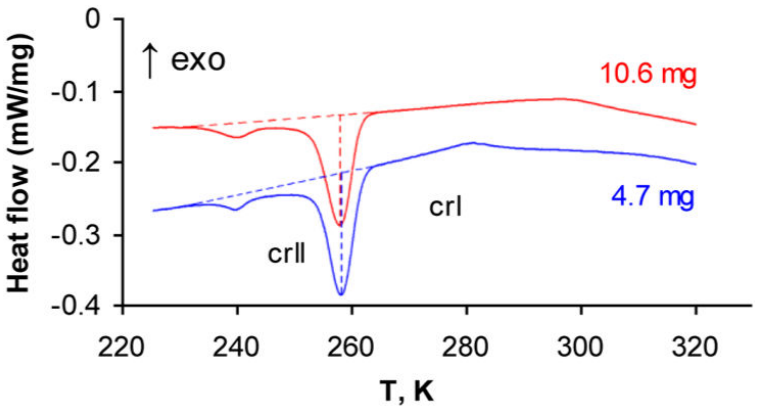

Figure 3.
DSC traces for two samples of APG (10.6 mg, top; 4.7 mg, bottom) showing the phase-transition region.

Table 1

Standard Thermodynamic Characteristics of Phase Transitions of L-Ala-L-Pro-Gly·H_2O Obtained by Adiabatic Vacuum Calorimetry

transition	temperature range (K)	T_{max} (K)	$\Delta_{tr}H_m$ (kJ·mol^{-1})	$\Delta_{tr}S_m$ (J·K^{-1}·mol^{-1})
crII ↔ crI	226–265	257.7 ± 0.5	2.944 ± 0.015	11.42 ± 0.06
anomaly	275–287	280.7 ± 0.5	0.0806 ± 0.0004	0.2873 ± 0.0014

Table 2

Standard Thermodynamic Characteristics of the crII ↔ crI Phase Transition of APG Obtained by DSC

sample mass (mg)	temperature range (K)	T_{max} (K)	$\Delta_{tr}H_m$ (kJ·mol^{-1})
10.6	228–263	257.7 ± 0.5	2.887 ± 0.014
4.7	228–263	257.9 ± 0.5	2.992 ± 0.015

Table 3

Calculated Molar Heat Capacities and Thermodynamic Functions of Crystalline L-Ala-L-Pro-Gly·H_2O at 0.1 MPa[a]

T (K)	$C_{p,m}$ (J·K^{-1}·mol^{-1})	$H(T) - H(0)$ (kJ·mol^{-1})	$S(T)$ (J·K^{-1}·mol^{-1})	$-[G(T) - H(0)]$ (kJ·mol^{-1})
		Crystal II		
5	0.235	0.000322	0.0783	0.0000977
10	1.79	0.00473	0.627	0.00149
15	6.26	0.0234	2.08	0.00782
20	13.50	0.07282	4.868	0.02455
25	22.66	0.1631	8.848	0.05817
30	32.37	0.3001	13.83	0.1148
35	42.52	0.4874	19.58	0.1980
40	52.79	0.7255	25.93	0.3115
45	62.63	1.014	32.72	0.4580
50	71.54	1.350	39.79	0.6394
60	89.18	2.154	54.39	1.110
70	106.6	3.133	69.45	1.729
80	122.9	4.281	84.76	2.500
90	137.5	5.585	100.1	3.424
100	150.2	7.025	115.3	4.501
110	162.1	8.587	130.1	5.728
120	174.1	10.27	144.8	7.103
130	186.1	12.07	159.2	8.623
140	197.2	13.99	173.4	10.29
150	208.8	16.01	187.3	12.09
160	222.5	18.17	201.3	14.03
170	235.1	20.46	215.1	16.11
180	246.6	22.87	228.9	18.34
190	258.0	25.39	242.5	20.69
200	269.8	28.03	256.1	23.19
210	282.2	30.79	269.5	25.81
220	292.6	33.67	282.9	28.58
230	302.3	36.64	296.1	31.47
240	312.0	39.71	309.2	34.50
250	321.7	42.88	322.2	37.65
260	331.4	46.15	335.0	40.94
265	336.3	47.82	341.3	42.63
		Crystal I		
265	336.3	50.76	352.4	42.63
270	341.9	52.46	358.8	44.41
273.15	345.8	53.54	362.7	45.55
280	354.7	55.94	371.4	48.06

T (K)	$C_{p,m}$ (J·K^{-1}·mol^{-1})	$H(T) - H(0)$ (kJ·mol^{-1})	$S(T)$ (J·K^{-1}·mol^{-1})	$-[G(T) - H(0)]$ (kJ·mol^{-1})
290	367.0	59.55	384.1	51.84
298.15	376.6	62.58	394.4	55.01
300	378.8	63.28	396.7	55.74
310	393.2	67.13	409.4	59.77
320	418.1	71.17	422.2	63.93
321	421.6	71.59	423.5	64.35

[a] Standard uncertainty of temperature $u(T) = 0.01$ K. Relative standard uncertainty of heat capacity $u_r(C_{p,m})$ is 0.02, 0.005, and 0.002 in ranges $6 \leq T \leq 15$ K, $15 \leq T \leq 40$, and $40 \leq T \leq 321$ K, respectively.